



HAL
open science

Evaluation of LoRa technology in 433-MHz and 868-MHz for underground to aboveground data transmission

Laure Moiroux-Arvis, Christophe Cariou, Jean-Pierre Chanet

► **To cite this version:**

Laure Moiroux-Arvis, Christophe Cariou, Jean-Pierre Chanet. Evaluation of LoRa technology in 433-MHz and 868-MHz for underground to aboveground data transmission. *Computers and Electronics in Agriculture*, 2022, 194, pp.106770. 10.1016/j.compag.2022.106770 . hal-03790419

HAL Id: hal-03790419

<https://hal.inrae.fr/hal-03790419v1>

Submitted on 22 Jul 2024

HAL is a multi-disciplinary open access archive for the deposit and dissemination of scientific research documents, whether they are published or not. The documents may come from teaching and research institutions in France or abroad, or from public or private research centers.

L'archive ouverte pluridisciplinaire **HAL**, est destinée au dépôt et à la diffusion de documents scientifiques de niveau recherche, publiés ou non, émanant des établissements d'enseignement et de recherche français ou étrangers, des laboratoires publics ou privés.



Distributed under a Creative Commons Attribution - NonCommercial 4.0 International License

1 Evaluation of LoRa technology in 433-MHz and 868-MHz 2 for underground to aboveground data transmission

3 Laure Moiroux-Arvis^{1*}, Christophe Cariou¹, Jean-Pierre Chanet¹

4 ¹ University Clermont Auvergne, INRAE, UR TSCF, F-63000 Clermont-Ferrand, France

5 * Corresponding author, laure.moiroux@inrae.fr

7 Abstract

8 The development of Wireless Underground Sensor Networks (WUSNs) is currently receiving significant attention to collect data underground all along the year without impacting
9 aboveground activities. Although the opportunities are promising for sectors as agriculture and environment monitoring, the task is particularly challenging as the radio waves are
10 significantly more attenuated in the soil in comparison with in the air. In addition, the communication ranges are highly impacted by some operating and environmental conditions
11 as the soil moisture, its composition and compaction as well as the burial depth of the nodes. In this paper, we developed two sets of nodes operating at 433 MHz and 868 MHz based
12 on the LoRa technology which is the physical layer of the Low Power Wide Area Network LoRaWAN and initially developed for aboveground IoT applications. We successively tested
13 these nodes in real conditions on underground to aboveground (UG2AG) data transmissions and with various operating conditions and radio parameters. First results highlighted the
14 interest of the 868 MHz radio modules tuned at the maximal allowed transmit power in Europe (+14 dBm/25 mW), in comparison with the 433 MHz radio modules (+10 dBm/10
15 mW). Next results enabled to point out the importance of the inclination of the receiving antenna but also the impact of the burial depth of the emitting node, as well as the interest to
16 place the emitting antenna directly in contact with the soil. The best configuration enabled to reach UG2AG ranges of more than 275 meters long with low depth buried nodes (15 to
17 30 cm), that clearly enables to envision agriculture and environment monitoring applications based on such radio modules.

18
19
20
21
22
23
24
25
26
27
28 **Keywords:** Wireless Underground Sensor Networks, IoUT, LoRa technology, environmental
29 monitoring, precision agriculture.

31 1 Introduction

32 In the coming years, Wireless Underground Sensor Networks (WUSNs) are expected to play
33 a major role in the environment monitoring and real time decision making (Sardar et al., 2019,
34 Sambo et al., 2020). The applications range from smart irrigation and precision farming to
35 minimize water losses and optimize the use of agricultural resources (Silva and Vuran, 2010)
36 to the detection of pesticide residues in soil near rivers (Akyildiz and Stuntebeck, 2006) and
37 early population warning against risks of landslides (Ferreira et al., 2019). Other potential
38 applications are underground infrastructure monitoring (e.g. pipes, storage tanks), sport field
39 monitoring and detection of people or vehicles aboveground (Zaman and Forster, 2018). These
40 applications are based on the development of nodes composed of sensors, radio communication
41 devices and antennas, all buried at a few dozens of centimeters deep to collect data directly

42 from the underground environment (e.g. moisture, temperature, salinity, vibrations) without
 43 impacting the aboveground activities and all along the year. The interest to conceal the nodes
 44 underground is also to protect them from potential damages caused by humans, animals and
 45 machines (Huang et al., 2020). The data collected in the field are next transferred to the cloud,
 46 leading to the new paradigm of Internet of Underground Things (IoUT) (Saeed and al., 2019,
 47 Salam and Raza, 2020).

48 As depicted on Figure 1, three communication links, called underground to underground
 49 (UG2UG), underground to aboveground (UG2AG) and aboveground to underground (AG2UG),
 50 are possible in a wireless underground sensor network (Silva et al., 2014). The establishment of
 51 the communication between the different nodes is however challenging as the radio electroma-
 52 gnetic waves are significantly more attenuated in the soil in comparison with in the air (20-300
 53 times worse) (Da Silva et al., 2014). In particular, the UG2UG link is difficult to obtain, the
 54 communication ranges reported in the literature being generally lower than a few meters. More-
 55 over, compared with in the air, many environmental factors affect the inter-node communication
 56 distance in a WUSN, especially the Volumetric Water Content (VWC) or soil moisture which
 57 drastically attenuates the propagation of the radio signals underground (Bogena et al., 2009). In
 58 UG2UG, the strength of the received signals can decrease of several dozens of decibel-milliwatts
 59 on wet soil compared to a dry soil (Vuran and Silva, 2009). The composition of the soil, i.e. the
 60 percentage of sand, silt and clay (Foth, 1990), impacts also indirectly the inter-node connectivity
 61 with greater or lesser water holding capacity. The topology of the terrain is also an important
 62 point to be considered to adequately place the nodes in the field, as well as the burial depth (i.e.
 63 the distance between the antenna and the surface) which impacts the strength of the received
 64 signal for the UG2AG/AG2UG links (Sambo et al., 2020), but also for the UG2UG links which
 65 are affected by the reflection of the radio waves by ground surface (Vuran and Silva, 2010). The
 66 roots of plants and trees as well as the stage of vegetation aboveground can also impact the
 67 UG2AG/AG2UG communications (Vuran and Silva, 2009). Several work aim to characterize,
 68 modelize and simulate the propagation of radio waves in soil face to such varying environmental
 conditions (Vuran and Akyildiz, 2010, Silva et al., 2015).

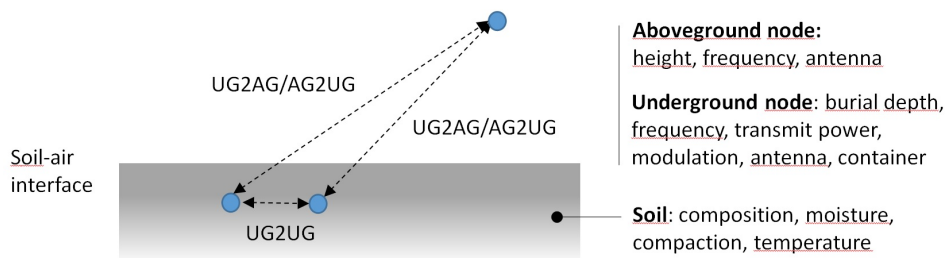


Figure 1: Communication links in WUSN and main influencing factors

69
 70 The choice of the operating frequency for the radio transceivers is also essential as the
 71 attenuation in soil increases with the frequency value. Several studies highlighted however
 72 that the 300-900 MHz frequency band is particularly relevant for WUSNs as it leads to higher
 73 communication ranges compared for example with the 2.4 GHz (Silva et al., 2015) and it enables
 74 to use reasonable sizes of antennas (a quarter of the signal wavelength). The antennas can be
 75 directly in contact with the soil or inside a container, and of different types (e.g. monopoles or

76 dipoles antennas) (Tiusanen, 2009, Salam et al., 2019). The maximum transmit power is limited
77 by the regulations in the country where the WUSNs are deployed. A compromise has also to be
78 found between the transmit power and energy consumption of the buried nodes to obtain run
79 times ideally for several months or years without battery replacement.

80 In Europe, the 433.05-434.79 MHz and 863-870 MHz are licence free bands particularly rele-
81 vant to develop WUSNs. They are already used for IoT applications by the Low Power Wide
82 Area Networks (LPWANs), as SigFox, NB-IoT and LoRaWAN, for sending small data packages
83 over long distances with low energy consumption on battery powered nodes. With its open pro-
84 tocol, the interest of LoRaWAN (LoRa Alliance, 2018) is its physical layer, the LoRa technology,
85 developed in 2014 by the French start-up company Cycleo and today managed by Semtech. This
86 technology is based on a Chirp Spread Spectrum (CSS) modulation technique, which encodes
87 information using frequency chirps having a linear variation of frequency over time (Augustin
88 et al., 2016). In the air, this modulation leads to a certain immunity against interferences and
89 multi-paths (Staniec and Kowal, 2018). Several LoRa radio modules are today off the shelf
90 at 433 MHz and 868MHz. In the regard of European regulations, 433 MHz transmissions are
91 allowed at +10 dBm/10 mW whereas 868 MHz transmissions are allowed at +14 dBm/25 mW
92 for the specific 868.0-868.6 MHz frequency band. In addition to the operating frequency and
93 transmit power, several parameters can be configured on the LoRa radio modules, in particular
94 the spreading factor (SF), the coding rate (CR) and the bandwidth (BW), see (Augustin et al.,
95 2016). A compromise has to be found between these parameters: high SF values lead to high
96 sensitivity and long communication range to the detriment of airtime and thus energy consump-
97 tion. High CR values lead to increase the robustness of transmission to the detriment of the
98 airtime and thus also energy consumption. High BW values lead to high data rate and short
99 airtime, but low sensitivity (Zorbas et al., 2018).

100 In the literature, still very few work have investigated the performance of LoRa communica-
101 tion for WUSNs in real conditions. In (Hardie and Hoyle., 2019), LoRa nodes operating at 433
102 MHz are buried in the soil from 15 to 30 cm deep with different combinations of LoRa para-
103 meters. The obtained transmission distances UG2AG with a transmit power of +25 dBm in SF
104 12 in relatively dry soil were about 100-200 m, depending on the chosen configuration and soil
105 composition. This work highlighted the difficulty to reach more than a few meters in UG2UG
106 that leads to question the interest of this link in an agricultural context. The issue of power
107 consumption for the buried node is also pointed out. In (Ebi et al., 2019), the radio transmission
108 performances in LoRa and LoRaWAN are evaluated at 868 MHz to monitor an underground
109 infrastructure. They highlighted the interest to first use the LoRa technology for the UG2AG
110 communication, in order to obtain reliable packet delivery, to next use the LoRaWAN protocol
111 for the aboveground communications. In (Lin et al., 2019), the link quality of the UG2AG LoRa
112 communication is investigated, in particular with respect to the burial depth and the internode
113 distance. No packet loss was observed if the RX node is located at the vicinity of the TX node,
114 even at the maximum burial depth (0.8 m). This was also the case with an internode distance of
115 50 m when TX nodes are buried at 0.4 m. For Tx nodes buried more deeply (0.6 m and 0.8 m),
116 the packet loss increased progressively with the internode distance to be total at respectively
117 28 m and 22 m. In (Gineprini et al., 2020), less than one percent of the transmitted packets

118 was lost with an UG2AG communication link composed of 27 m aboveground and from 0.1 m
 119 to 0.5 m underground. In (Di Renzone et al., 2021), the performances of data transmission in
 120 LoRaWAN for different soil compositions was studied for depths up to 0.5 m. The packet loss
 121 was below 2 % whatever the soil composition with the gateway placed at 15 m. In (Wu et al.,
 122 2019), a simulator was developed to study the impact of soil moisture and burial depth on a
 123 LoRaWAN network with a centre frequency ranging from 915 to 928 MHz in New Zealand.

124 Although UG2UG links are difficult to establish, the UG2AG links with a star topology
 125 can be sufficient for numerous applications. This is the case for example of sensors and nodes
 126 deployed underground with aboveground collector and repeater nodes. The UG2AG link must
 127 however be robust and well-designed. The objective of this paper is to first compare the per-
 128 formance of LoRa technology at both 433 MHz and 868 MHz frequency bands for this UG2AG
 129 link and next establish an adequate configuration, in particular in terms of burial depth, incli-
 130 nation of the receiving antenna and contact of the emitting antenna with the soil, with the aim
 131 to develop future environmental and agricultural monitoring applications. For that, the nodes
 132 were built from commercial components. The maximum transmit powers authorized in Europe
 133 for each of the frequency bands were used. The experiments were carried out with a spreading
 134 factor (SF) ranging from 7 to 12 to highlight the impact of this parameter on the attainable
 135 communication range. The impact of the soil moisture on the UG2AG communication range
 136 was first studied to determine the preferred choice for the frequency band for the UG2AG link.
 137 Next, the impacts of the burial depth, the inclination of the receiving antenna and the way to
 138 bury the emitting antenna were investigated, as well as the analysis of the packet loss.

139 2 Experimental setup

140 2.1 Presentation

141 The experimentations reported in this paper follow the scheme presented on Figure 2.

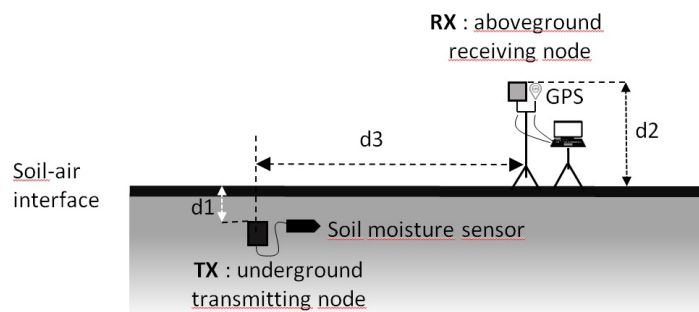


Figure 2: Experimental setup

142 A soil moisture sensor is buried at the deep d_1 in an open field. This sensor is connected to an
 143 underground node TX transmitting periodically the data of the probe (humidity, temperature,
 144 dielectric permittivity) in LoRa to a receiving node RX located aboveground at the height d_2
 145 and a varying distance d_3 : the RX node is moved until the UG2AG link is disrupted. The data
 146 frame are recorded on a computer which is connected to a GPS to georeference the successive
 147 positions. First experiments use a set of TX and RX nodes operating at 433 MHz, and second

148 experiments use a set of TX and RX nodes operating at 868 MHz. The power of the radio
 149 transmitters are tuned to the maximum value allowed by the European regulations, respectively
 150 +10 dBm/10 mW and +14 dBm/ 25mW. On a periodic basis (every 12 s), the TX node picks
 151 up the measured values from the sensor and sends a set of six frames with the LoRa parameter
 152 SF going from 7 to 12. The RX node waits several minutes on a position enabling to receive
 153 several sets of six frames. These experimentations are repeated with different soil moistures,
 154 burial depths, RX antenna inclinations and with the TX antenna directly in contact with the
 155 soil or inside a PVC container.

156 2.2 Materials

157 A first set of TX and RX nodes is built with RFM98W radio modules operating at 433
 158 MHz. A second set uses RFM95W radio modules operating at 868 MHz. These radio modules
 159 are manufactured by HopeRF and include the SX1276 transceiver from Semtech with the LoRa
 160 technology. The TX nodes, see Figure 3, are composed of a microprocessor ATmega328 running
 161 at 8 MHz installed on an Arduino Pro Mini board and a radio module RFM98W/95W with a
 162 quarter wave whip antenna (RF FLEXI-SMA90-433, 2 dBi gain, 16.2 cm at 433 MHz and RF
 163 FLEXI-SMA-868, 2 dBi gain, 13.6 cm at 868 MHz). The radiation pattern of these antennas
 164 is maximum at perpendicular to the whip and close to zero at the end. They will be vertically
 165 oriented in the experiments. The TX node is powered with a 3.6 V/8800 mAh Lithium-Ion
 166 battery, and connected to a Truebner SMT100 probe. The RX nodes, see Figure 4, are composed
 167 of a microprocessor ATmega328 running at 8 MHz installed on an Arduino Pro Mini board and
 168 a radio module RFM98W/95W with a quarter wave whip antenna (Siretta Delta 12A, 3 dBi
 169 gain, 13 cm at 433 MHz and Taoglas TI.18.3113, 3.2 dBi gain, 39 cm at 868 MHz). The supply
 170 of the RX node is delivered by the USB port of the computer on which it is connected.

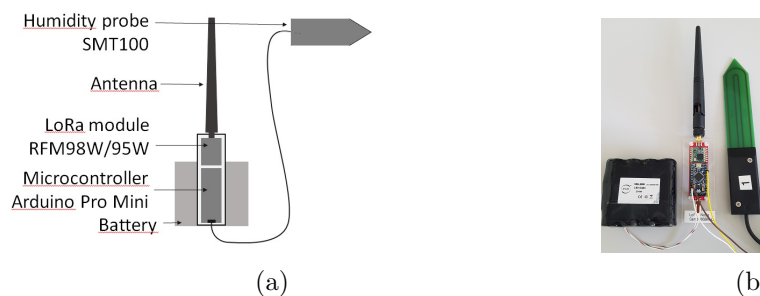


Figure 3: Transmitter node TX: a) Sectional drawing b) Battery, node and moisture probe



Figure 4: Receiver node RX: a) Principle scheme, b) Node, c) GPS (u-blox C94-m8p)

171 2.3 Software development

172 The Arduino Pro Mini boards of the TX nodes are programmed to configure the parameters
 173 of the radio module LoRa (frequency, transmit power, spreading factor SF, coding rate CR,
 174 bandwidth BW) and periodically transmit the data frame presented on Table 1.

Table 1: Data frame (15 bytes) sent by the TX node to the RX node

Name	Description
Node ID	Node identifiant
SF	Spreading factor (varying from 7 to 12)
Counter	Number of the frame
Permittivity	Data of the sensor SMT100
Humidity	Data of the sensor SMT100
Temperature	Data of the sensor SMT100

175 Different values for the spreading factor SF are used in order to experimentally quantify
 176 its impact on the communication range. Theoretically, the higher it is, more the range increases
 177 but to the detriment of the data rate as the signal is transmitted over a longer period of time,
 178 see Table 2, but also to the detriment of the energy consumption as the radio communication
 179 is longer. At each cycle, the TX node reads the data of the SMT100 probe and successively
 180 transmits six frames with a spreading factor SF varying from 7 to 12, see the diagram of the
 181 TX program on Figure 5a. The output power is constant and tuned at +10 dBm for the 433
 182 MHz node and +14 dBm for the 868 MHz node. The coding rate CR is equal to 4/5 and the
 183 bandwidth BW is tuned to 125 KHz.

Table 2: Transmit time of a frame of 15 bytes with respect to the SF value. BW = 125 KHz, CR = 4/5. Values given by the application "LoRa Modem Calculator Tool" from Semtech.

Spreading factor	RF transmit time (ms)	SNR required (dB)
SF=12	933.9	-20
SF=11	466.9	-17.5
SF=10	299.0	-15
SF=9	149.5	-12.5
SF=8	74.8	-10
SF=7	45.6	-7.5

184 The RX node waits for data from the TX node. To establish a communication, the value
 185 of the spreading factor SF must be identical for both the TX and RX nodes. The RX node
 186 is initialized at SF=7 and scans until the reception of a frame, see the diagram of the RX
 187 program on Figure 5b. At each received frame, the RX node reads the values RSSI (Received
 188 Signal Strength Indication) and SNR (Signal-to-noise Ratio) which qualify the RF signal. It
 189 concatenates then the received frame of the TX node and the values of the RF signals to next
 190 send this frame to the computer, see Table 3. On the computer, a program in Python reads
 191 the data frames and stores them in a dated file with the GPS position. These data are next
 192 processed and analysed using Matlab software.

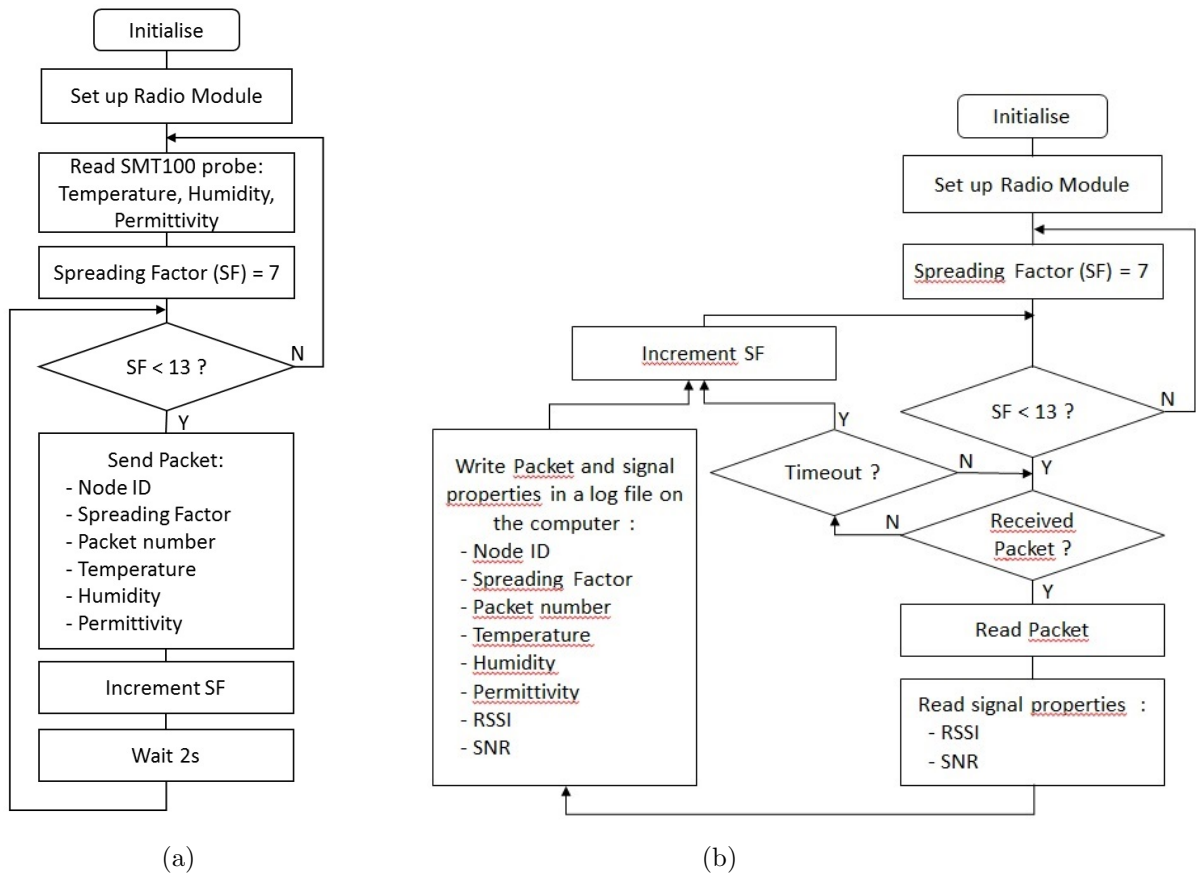


Figure 5: Diagrams of the program in the: (a) TX node, (b) RX node

Table 3: Data frame sent by the RX node to the computer

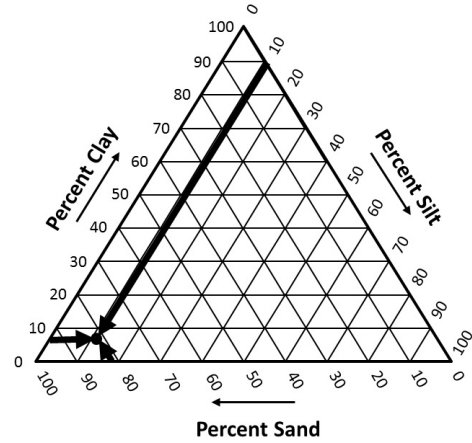
Name	Description
Node ID	Node identifier
SF	Spreading factor detected
Counter	Number of the frame
Permittivity	Data of the sensor SMT100
Humidity	Data of the sensor SMT100
Temperature	Data of the sensor SMT100
RSSI	Received Signal Strength Indication
SNR	Signal-to-noise Ratio

193 3 Experimentations

194 The experiments were carried out at the experimental field of INRAe (French National
 195 Research Institute for Agriculture, Food and Environment) presented on Figure 6. This field
 196 of 3.8 hectares is an open environment, flat without obstacles. At low depth, the composition
 197 of the soil is 81.6 % of sand (72.3 % of fine sand and 9.3 % of coarse sand), 11.3 % of silt
 198 (7.1 % of fine silt and 4.2 % of coarse silt) and 7.1 % of clay. The weather conditions were low
 199 temperatures (respectively 7.6 °C and 8.7 °C) with cloudy sky.



(a)

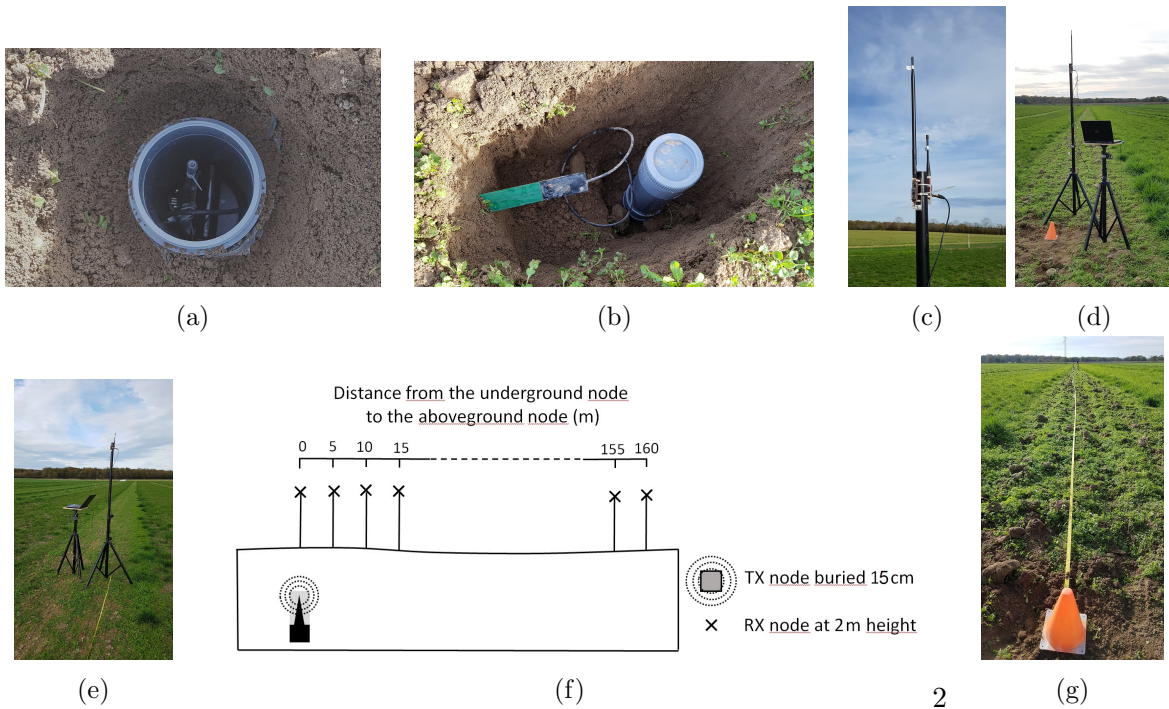


(b)

Figure 6: Experimental field: (a) Google Earth © Digital Globe, 46°20'22.35"N, 3°25'44.28"E, 280m (b) Soil texture triangle based on the Unites States Department of Agriculture (USDA) classification

200 3.1 Tests with different soil moistures

201 A PVC tube of 8 cm diameter is buried on the field with the moisture probe on the side,
 202 see Figures 7a and b. It is next covered with soil and compacted. A first set of experiments
 203 uses a set of TX and RX nodes operating at 433 MHz. A second set of experiments uses nodes
 204 operating at 868 MHz. Two different soil moistures (10 % and 22 %) are investigated. For each
 205 experiment, the TX node is installed inside the tube at about $d_1 = 15$ cm deep. The RX node
 206 is positionned on a tripod at $d_2 = 2$ m height, see Figures 7c, 7d, 7e, and is straightly moved
 207 with steps of 5 m, see Figures 7f anf 7g.



(a)

(b)

(c)

(d)

(e)

(f)

2

(g)

Figure 7: Testbed: (a,b) The TX node is buried with the probe at 15 cm depth, (c,d,e) The RX node is installed on a tripod at 2 m height, (f,g) Steps of 5 m are carried out.

208 In the first set of experiments, the soil moisture is measured by the probe at 10.3 %, the
 209 soil relative permittivity at 6.0 and the soil temperature at 9.4 °C. The results are presented on
 210 the left part of Figure 8: at each inter-node distance RX-TX, the SF graphics highlight if the
 211 UG2AG link was successfully established or not for a spreading factor SF varying from 7 to 12.
 212 Clearly, the set of nodes operating at 868 MHz reached longer distance (170 m) than with the
 213 set at 433 MHz (125 m). These distances were reached by configuring a high spreading factor
 214 (SF 12) for the LoRa modules, that enables a high sensitivity and communication range to the
 215 detriment of the airtime and high energy consumption. We can observe that until 90 m, the
 216 UG2AG link at 868 MHz is maintained for all the SF values, whereas only 55 m for the UG2AG
 217 link at 433 MHz. Therefore, although the 433 MHz is theoretically more relevant to obtain longer
 218 communication range compared with the 868 MHz, the possibility to tune higher the power
 219 transmit at 868 MHz (+14 dBm for the 868 MHz and +10 dBm for the 433 MHz in line with
 220 the regulations) reverses the results. The values RSSI (Received Signal Strength Indication)
 221 and SNR (Signal-to-Noise Ratio) of the RX node decrease slowly with respect to the internode
 222 distance. They are however clearly higher at 868 MHz than at 433 MHz enabling to maintain
 223 the communication at a longer distance, despite more variations at 868 MHz.

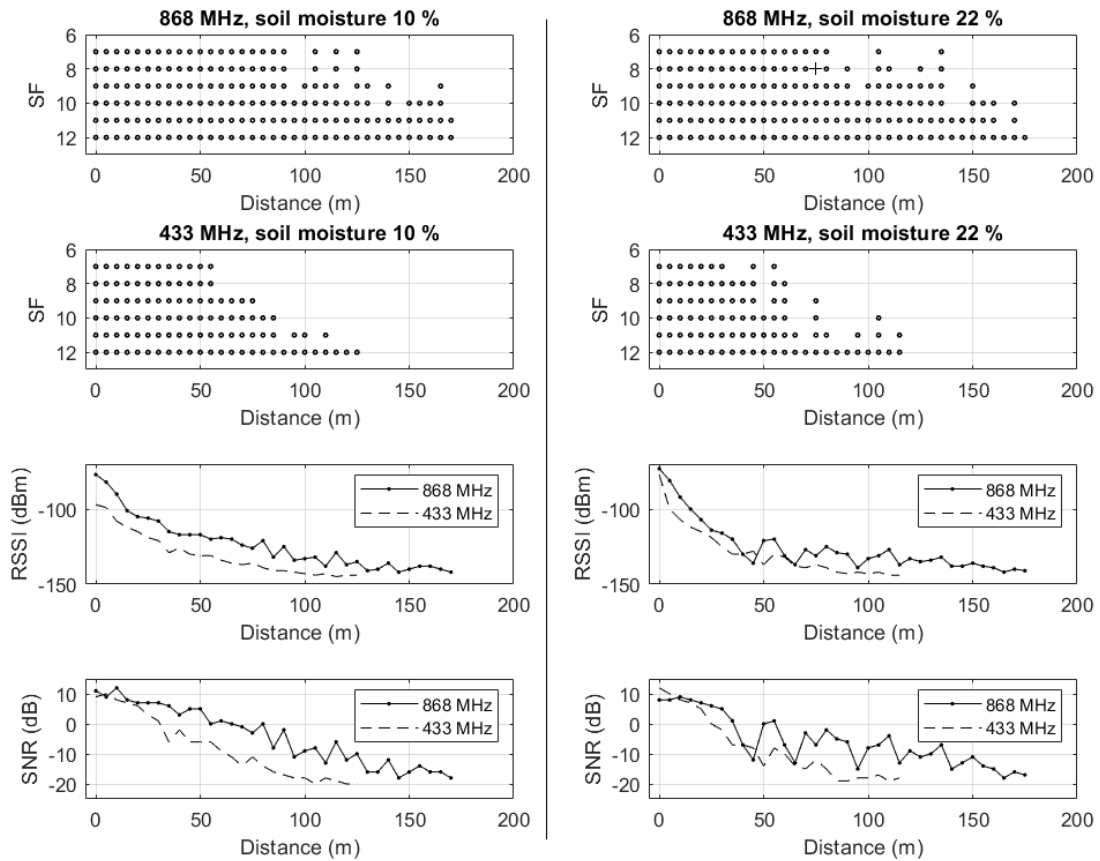


Figure 8: Measurements on the UG2AG link obtained with a soil moisture of respectively 10 % (left part) and 22 % (right part)

224 In the second set of experiments, the soil moisture and permittivity were doubled in compa-
 225 rison with the first experiments (soil moisture 22.8 % and relative permittivity 12.2). The soil
 226 temperature was at 11.9 °C. The results are presented on the right part of Figure 8. We can

227 observe that the maximal internode distance with the set of nodes at 868 MHz is slightly affected
 228 by the higher soil moisture, leading to communications until 175 m. Moreover, until 80 m, the
 229 communications are always possible with all the SF values. The set of nodes at 433 MHz is
 230 however more impacted by the higher soil moisture: the maximal internode distance is slightly
 231 reduced (from 125 m to 115 m) but the communications are only possible with high SF values,
 232 and that from the distance 70 m. The RSSI and SNR values are however more stable at 433
 233 MHz than at 868 MHz which have more variations.

234 For these tests, we can also notice that the minimal RSSI value for the RX node is measured
 235 at -144 dBm, that is close to the sensitivity given in the datasheet of the SX1276 component
 236 (-148 dBm). These experiments highlight the importance of this parameter in the choice of
 237 the radio component. By comparison, the sensitivity of the first LoRa transceiver SX1272 from
 238 Semtech was -137 dBm. In addition, these experiments highlight that as the communication
 239 signal is less attenuated at 868 MHz than at 433 MHz, a lower SF can be used to reach the same
 240 distance (e.g. at 100 m and soil moisture 22.8 %, the TX node at 868 MHz can use a SF=9
 241 whereas the TX node at 433 MHz has to use a SF=12). That enables to reduce the transmit
 242 time (this time is divided by six from SF=12 to SF=9, see the previously presented Table 2),
 243 and therefore limit the energy consumption of the TX node.

244 3.2 Tests with the same transmit power (10 mW)

245 The previous tests were carried out with TX nodes in line with the European regulations, i.e.
 246 +14 dBm/25 mW at 868 MHz and +10 dBm/10 mW for the 433 MHz, meaning a difference of
 247 4 dBm. To compare the performances with the same transmit power, the transmit power of the
 868 MHz TX node was decreased at +10 dBm/10 mW. The results are presented on Figure 9.

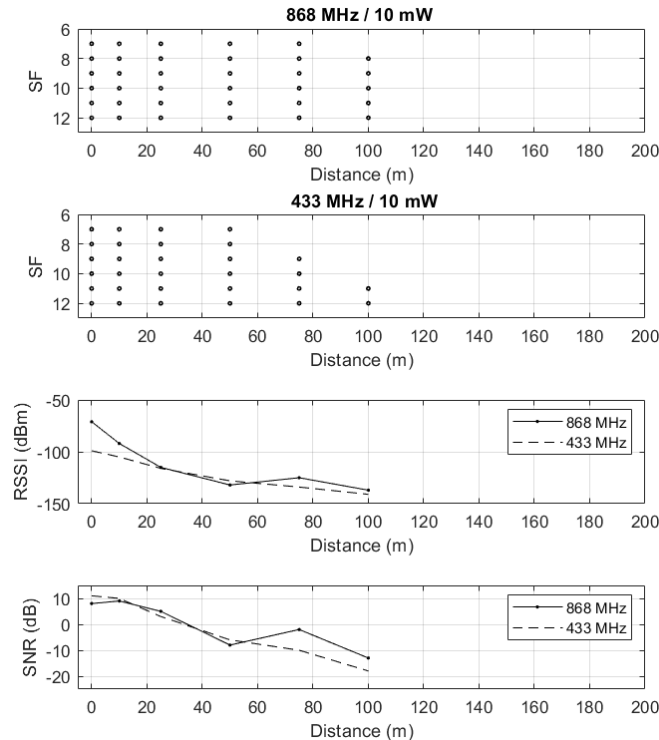


Figure 9: Same transmit power

248 We can observe that, even with the same transmit power, the communication at 868 MHz
 249 is less attenuated than at 433 MHz (e.g. at the distance of 100 m, the signal is received at 868
 250 MHz with SF=8 and SNR=-13 dB whereas at 433 MHz the signal is received with SF=11 and
 251 SNR=-18 dB).

252 Face to such results, we decided to continue the investigations on the UG2AG communication
 253 link using exclusively the 868 MHz frequency band. We investigated different configurations for
 254 the deployment of the nodes which can impact the communication range. The following section
 255 addresses the impact of the inclination of the RX antenna on the communication range.

256 3.3 Tests with different RX antenna inclinations

257 The objective is here to study the impact of the inclination of the RX antenna on the
 258 communication range, see Figures 10a and 10b. Preliminary tests enabled to select two relevant
 259 inclinations of the RX antenna for the field experiments, i.e. a vertical RX antenna and an
 260 inclined RX antenna at 45° . The RX antenna is pointed towards the buried TX node. As
 261 previously, the TX node is placed in a PVC tube and buried at 15 cm deep. The RX node
 262 is placed at 2 m above the soil. The experimental conditions were permittivity 9.0, humidity
 263 16.85 %, temperature 6.8°C .

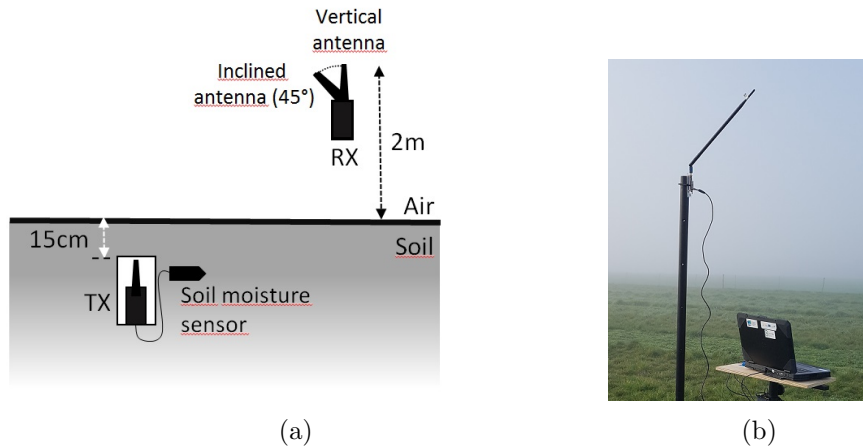


Figure 10: a) Experimental setup, b) Inclination of the Rx antenna pointed toward the TX node

264 The results are presented on Figure 11. They highlight that the inclination of the RX
 265 antenna enables to maintain the communications with low SF (e.g. at 250 m, SF=9 when the
 266 RX antenna is inclined, and SF=12 when the RX antenna is vertical) and significantly reduce
 267 the attenuation of the signal: the RSSI signal is about 10 to 15 dBm higher when the RX
 268 antenna is inclined in comparison when the RX antenna is vertical. The SNR signal remains
 269 moreover positive on a distance largely superior when the RX antenna is inclined (positive until
 270 150 m) in comparison when the RX antenna is vertical (positive until 50 m).

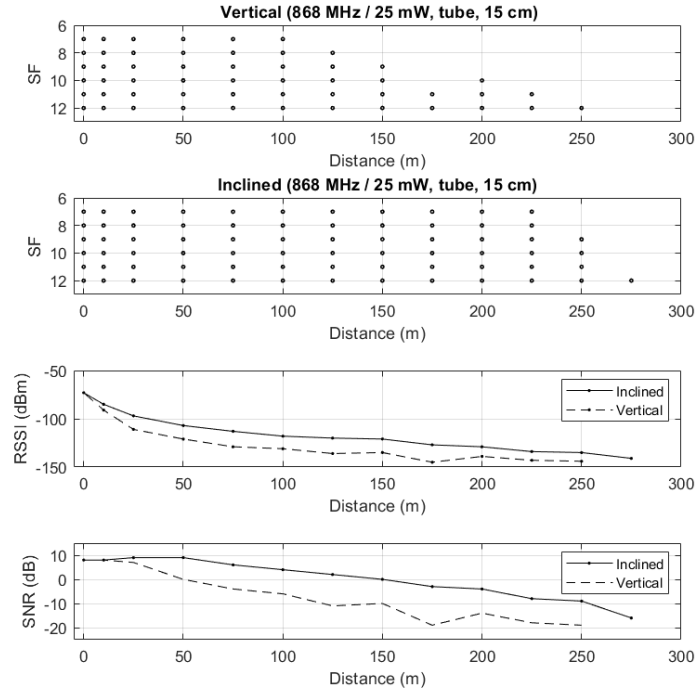


Figure 11: Tests with a vertical and inclined (45°) RX antenna

271 3.4 Tests with different burial depths for the TX node

272 After have highlighted the interest of the 868 MHz frequency band and the inclination of
 273 the RX antenna, the objective of the following experimentations were to evaluate the impact
 274 of the depth of the buried node on the UG2AG communication. For that, two burial depths
 275 were considered, respectively 15 cm and 30 cm as depicted on Figure 12. The RX node is still
 276 placed at 2 m above the soil, and the measurements are carried out successively with a vertical
 277 RX antenna and an inclined RX antenna. The experimental conditions were permittivity 12.45,
 humidity 23.36 %, temperature 8.7 °C. The results are presented on Figure 13.

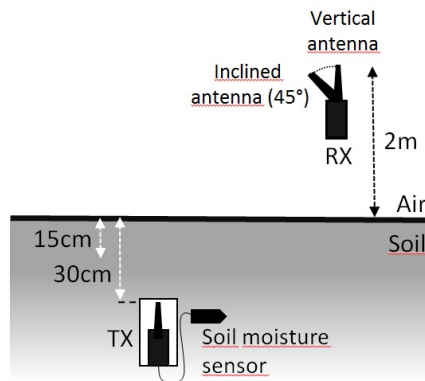


Figure 12: Experimental setup

278
 279 When the RX antenna is vertical, the communication range was 250 m when the TX node is
 280 at 15 cm deep. At 30 cm deep, the range is reduced to 175 m. The values of RSSI and SNR are
 281 however similar until 175 m, but when the TX node is at 15 cm, the RSSI signal is maintained

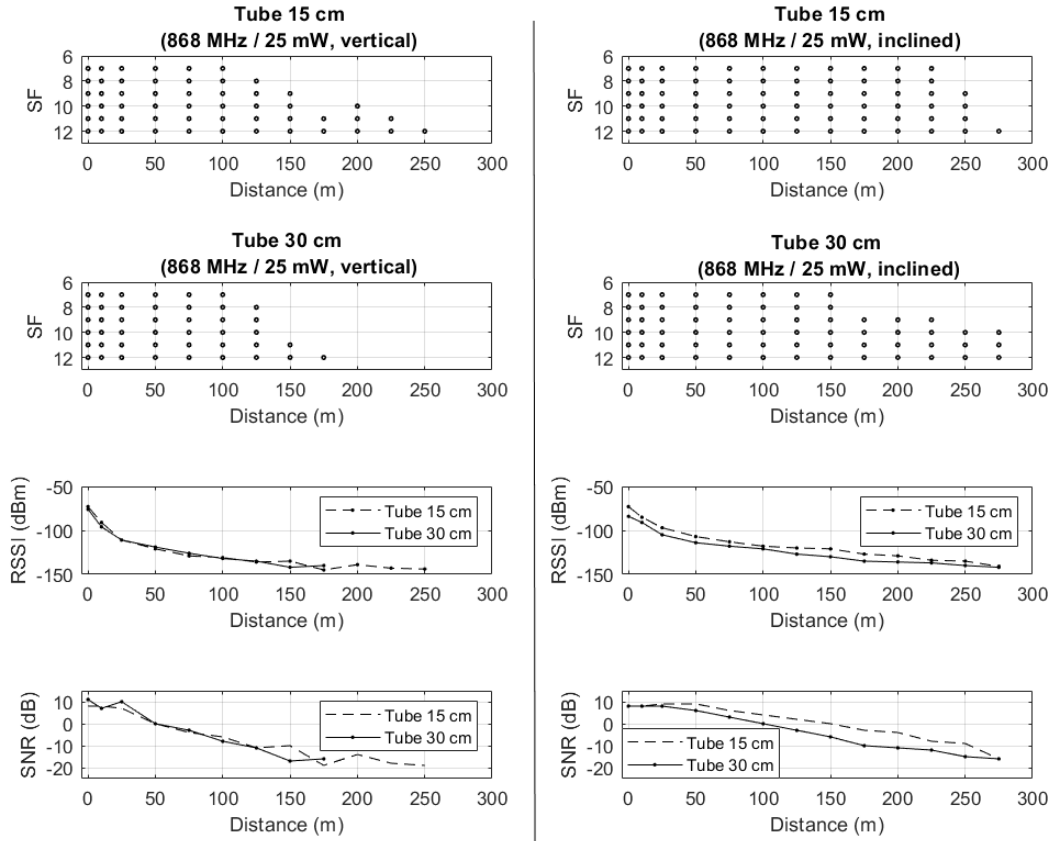


Figure 13: Measurements on the UG2AG link obtained with a burial depth of respectively 15 cm and 30 cm with a vertical RX antenna (left part) and inclined RX antenna (right part)

282 about -142 dBm until 250 m. When the RX antenna is inclined, the RSSI signal decreases of
 283 about 7dBm when the TX node is at 30cm deep in comparison with 15 cm. The SNR signal is
 284 positive until 100 m for the TX node at 30 cm deep, and until 150 m for the TX node at 15 cm
 285 deep (in comparison, the SNR signal is only positive until 50 m for the two burial depths when
 286 the Rx antenna is vertical). These results highlight the negative impact on the UG2AG link
 287 of the burial depth. However, the performances remain acceptable, even at 30 cm deep, that
 288 enables to envision environmental and agricultural monitoring applications.

289 3.5 Tests with the Tx antenna inside a container (PVC tube) or directly in 290 contact with soil

291 In all the experimentations presented in the previous sections, the TX antenna was located
 292 inside a PVC tube of 8 mm diameter. However, in order to check if this container had an
 293 impact on the quality of the communication, some comparative tests were carried out with
 294 the TX antenna directly in contact with the soil and the TX antenna in the PVC tube, see
 295 the principle scheme and materials on Figure 14. For each of these two configurations, the
 296 measurements were carried out with respectively 15 cm and 30 cm burial depths, and with
 297 respectively a vertical and inclined RX antenna. The experimental conditions were permittivity
 298 12.45, humidity 23.36 %, temperature 8.7 °C. Figures 15 and 16 present the results, and Tables
 299 4 and 5 highlight particular points.

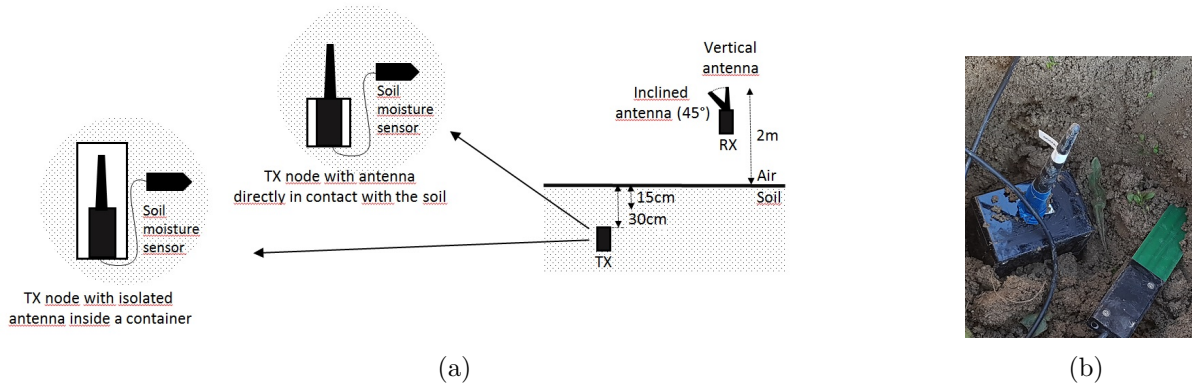


Figure 14: a) Experimental setup b) TX antenna directly in contact with the soil

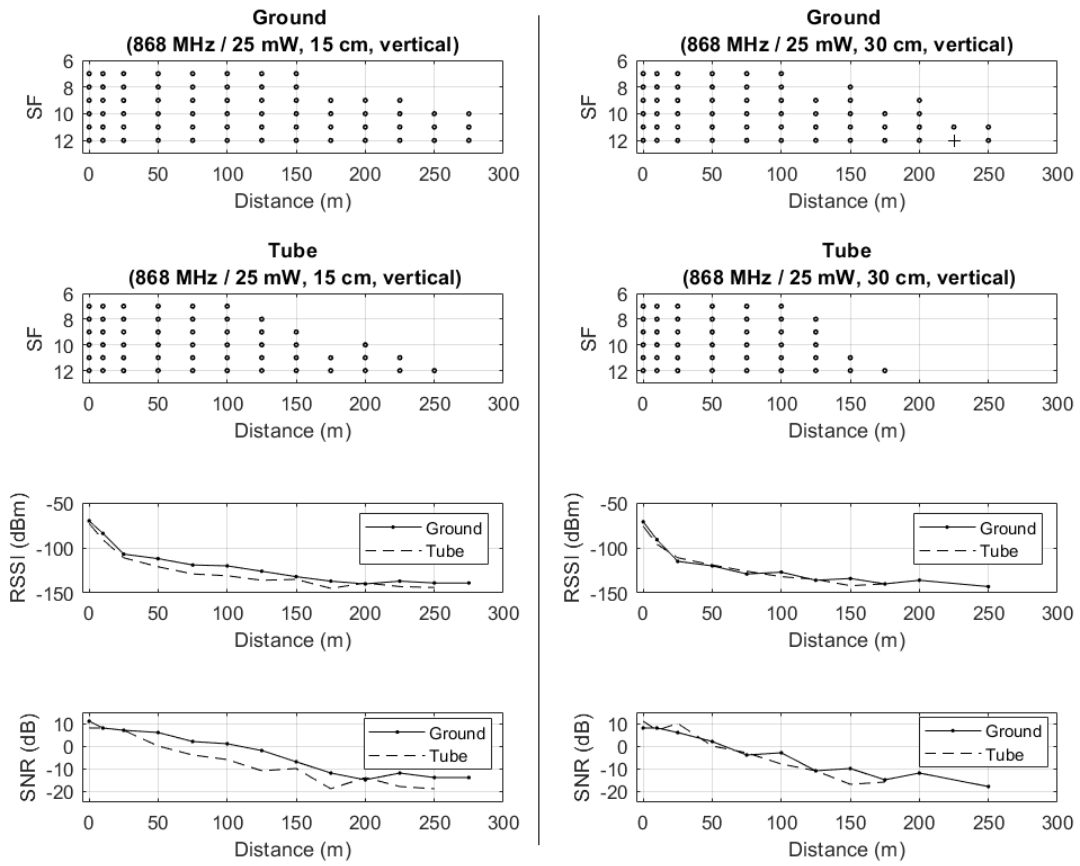


Figure 15: With vertical RX antenna

Table 4: Vertical RX antenna: RSSI and SNR values

		150 m		250 m	
		RSSI (dBm)	SNR (dB)	RSSI (dBm)	SNR (dB)
15 cm	Ground	-132	-7	-139	-14
15 cm	Tube	-135	-10	-144	-19
30 cm	Ground	-134	-10	-	-
30 cm	Tube	-142	-17	-	-

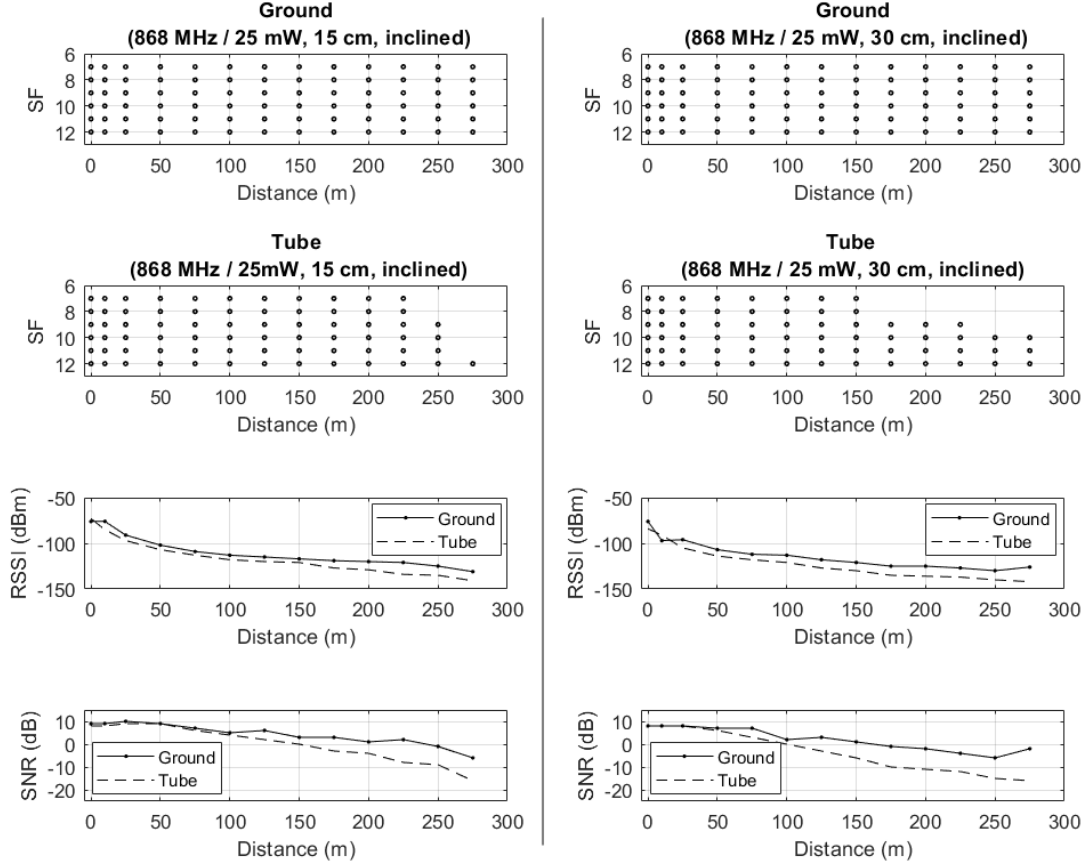


Figure 16: With inclined RX antenna

Table 5: Inclined RX antenna (45°): RSSI and SNR values

		150 m		250 m	
		RSSI (dBm)	SNR (dB)	RSSI (dBm)	SNR (dB)
15 cm	Ground	-117	3	-125	-1
15 cm	Tube	-121	0	-136	-10
30 cm	Ground	-120	2	-130	-6
30 cm	Tube	-130	-6	-140	-15

300 The RX antenna was vertical in Table 4, and inclined in Table 5. In the two Tables, the
301 results are given for the inter-node distances of respectively 150 m and 250 m. In Table 4, at
302 150 m, the RSSI value decrease of 3 dBm at 15 cm deep when the TX antenna is placed on
303 the PVC tube (from -132 to -135 dBm), and 8 dBm at 30 cm deep. At 250 m, the RSSI signal
304 is attenuated of 5 dBm at 15 cm deep, and no communication is possible at 30 cm deep. In
305 Table 5, it appears clearly that the RSSI and SNR values are improved when the RX antenna
306 is inclined. In particular, at 150 m, the SNR value remains positive when the RX antenna is
307 directly in contact with the soil at 15 cm and 30 cm.

308 These results highlight clearly the negative impact of the PVC container on the communica-
309 tion. The performances are better when the TX antenna is directly in contact with the soil with
310 RSSI signals about 10 dBm higher. Moreover, when the RX antenna is inclined and the burial

311 depth is 15 cm with the TX antenna in contact with the soil (see the right part of Figure 16),
 312 this configuration enables to emit with SF=7 whatever the distance, leading to a short transmit
 313 time and energy consumption. The attainable communication range with this configuration was
 314 275 m. However, the limit of the communication range was not reached and longer distance
 315 could certainly be attainable. In fact, at 275 m, we reached the limit of the experimental field.
 316 However, such distance is already suited to develop monitoring applications based on UG2AG
 317 communications.

318 3.6 Reliability of data transmission

319 The packet delivery ratio (PDR), i.e. the ratio between the number of received packets (R)
 320 to the total number of sent packets (S), is an indicator of the reliability of the communication,
 321 see (1).

$$PDR(\%) = \frac{R}{S} \cdot 100 \quad (1)$$

322 Experimentations were carried out to determine this ratio at each SF for internode distances
 323 going from 50 m to 200 m, see Table 6. The TX node was buried at 15 cm depth with the
 324 antenna directly in contact with the soil, and the RX node was located 2 m above the ground
 325 with a vertical RX antenna. At each SF, the TX node sends 100 packets and the number of
 326 received packets by the RX node was measured as well as the RSSI value.

Table 6: Packet delivery ratio at different SF and RSSI values. Experimental conditions are 868MHz /
 25mW, burial depth 15 cm, TX antenna in contact with the soil, vertical RX antenna, soil moisture
 17 %

RSSI	-115 dBm	-120 dBm	-130 dBm	-135 dBm
Internode distance	50 m	100 m	150 m	200 m
SF=7	99 %	100 %	9 %	0 %
SF=8	99 %	99 %	30 %	0 %
SF=9	100 %	97 %	90 %	37 %
SF=10	99 %	97 %	100 %	42 %
SF=11	100 %	100 %	100 %	90 %
SF=12	99 %	100 %	100 %	100 %

327 The results highlight that for RSSI values up to -120 dBm, that corresponds to an internode
 328 distance of 100 m, less than 3 % of packets were lost and the value of SF has little impact.
 329 However, from RSSI values below -130 dBm, the value of SF significantly impacts the quality
 330 of the link. At SF=7 and -130 dBm, only 9 % of the packets transmitted were received in
 331 comparison to 100 % at SF=12. At -135 dBm, no packet was received at SF=7 and still 100 %
 332 at SF=12.

4 Discussion and conclusions

This paper addresses the issue of the communication range of an UG2AG link in a WUSN to serve as basis for future applications in agriculture and environment monitoring. Based on the LoRa technology, two sets of nodes at 433 MHz and 868 MHz were built and tested in real conditions, i.e. an open field with sandy soil composition, soil moisture of 10 % and 22 %, and burial depth of the nodes at 15 cm and 30 cm. The interest of the 868 MHz radio modules at the maximal allowed transmit power in Europe (+14 dBm/25 mW) was first clearly highlighted with results more relevant in comparison to the 433 MHz frequency at +10 dBm/10 mW. Next, completed with a TX antenna directly placed in contact with the soil, as it was shown that a PVC container significantly attenuates the communication signal, and with an inclined RX antenna at 45° pointed toward the buried node, UG2AG communication ranges of more than 275 meters long were reached. At this distance, the LoRa parameter SF can moreover be maintained at a low value enabling to limit the energy consumption of the buried TX node. The benefit to place the TX antenna directly in contact with the soil and incline the RX antenna is highlighted in the Table 7 which is the synthesis of the results at the internode distance of 100 m.

Table 7: Synthesis of results at 868 MHz / 25 mW, internode distance: 100 m

RX antenna		Straight				Inclined			
TX antenna		Inside tube		Soil contact		Inside tube		Soil contact	
Burial depth (cm)		15	30	15	30	15	30	15	30
SF=7	RSSI (dBm)	-131	-132	-122	-129	-117	-123	-112	-115
	SNR (dB)	-7	-9	0	-6	4	-1	7	5
SF=8	RSSI (dBm)	-131	-132	-119	-131	-117	-123	-112	-115
	SNR (dB)	-7	-9	0	-7	4	-1	8	6
SF=9	RSSI (dBm)	-131	-133	-119	-129	-117	-124	-112	-115
	SNR (dB)	-7	-11	0	-6	5	-1	7	7
SF=10	RSSI (dBm)	-132	-132	-119	-129	-116	-121	-112	-114
	SNR (dB)	-7	-9	1	-6	4	0	7	7
SF=11	RSSI (dBm)	-131	-131	-120	-129	-117	-121	-112	-115
	SNR (dB)	-6	-7	1	-5	5	0	8	7
SF=12	RSSI (dBm)	-131	-132	-120	-129	-118	-121	-112	-115
	SNR (dB)	-6	-9	1	-5	4	0	8	7

Although these results are already relevant to envision the deployment of such nodes in the field, several improvements could be considered in future work. First, it will be necessary to deploy several TX buried nodes in the field during several seasons to study the behavior and reliability of the communications over different weather conditions and vegetation cover. Moreover, it could be interesting to adapt some parameters of the nodes, as well as the layout of the RX node in the field. In particular, the SF parameter could be tuned with respect to the soil moisture measured by the probe (e.g. low value in dry soil and high value in wet soil). Another way could be to modify the SF value with respect to the RSSI and SNR values measured by the RX node as with the adaptive data rate (ADR) in the LoRaWAN protocol (Li et al., 2018). This approach requires however to implement the AG2UG link and define

358 listening windows for the RX node. During our experiments, we have also observed the benefit
359 for the communication range to orientate the antenna of the RX node towards the TX node.
360 In case of several TX nodes disseminated in the field or a mobile RX node embedded on a
361 vehicle, an approach could be to actuate the orientation of the RX antenna to control and
362 maintain this direction during inter-node communications, e.g. from the knowledge of the GPS
363 coordinates. This approach requires however some memory capacities of the TX nodes and bi-
364 directionnal communications with adequate strategies. **Another point that could be considered**
365 **is to investigate the robustness of the UG2AG communication face to the potential presence of**
366 **interferences. In fact, the experimentations reported in this paper were performed in relatively**
367 **interference-free areas, i.e. without active transmitters in the immediate vicinity with the same**
368 **frequency range. Most of the time, this is the case in the considered applications (agriculture**
369 **and monitoring of natural environments). However, although LoRa is a robust technology**
370 **which possesses a remarkable immunity to multipath and interferences, in particular when small**
371 **bandwidths and high spreading factors are used, the presence of interferences in more disturbed**
372 **environmenst could be studied, with the possibility to adapt both the channel frequency and**
373 **the coding rate.** Finally, other frequency bands could also be advantageously investigated in
374 the WUSN, as the 869.4 - 869.65 MHz which allows transmit powers of 500mW, that means
375 twenty times higher than the transmit power used in this paper. This band is not part of the
376 LPWAN (Low Power Wide Area Networks) and is thus not suited for monitoring applications
377 as it would involve a high energy consumption for the TX buried node, but it could be used as
378 an alternative to send alert messages requiring reliable communications.

379 **Acknowledgement:** This work was sponsored by a public grant overseen by the
380 French National Research Agency as part of the “Investissements d’Avenir” through the IDEX-
381 ISITE initiative CAP 20-25 (16-IDEX-0001). The authors thank the ConnecSenS community,
382 the Federation of environmental research (FRE), and the employees of the National Research
383 Institute for Agriculture, Food and Environment (INRAE) who were involved in this work.

384 References

- 385 Akyildiz I. F., Stuntebeck E. P., 2006. Wireless underground sensor networks: Research chal-
386 lenges. *Ad Hoc Networks* 4, 669-686.
- 387 Augustin A., Clausen T., Townsley W.M., 2016. A study of LoRa: long range and low power
388 networks for the Internet of Things. *Sensors*, 16, 1466; doi:10.3390/s16091466.
- 389 Bogena H. R., Huismana J. A., Meierb H., Rosenbauma U., Weuthena A., 2009. Hybrid wireless
390 underground sensor networks: quantification of signal attenuation in soil. *Vadose Zone Journal*,
391 8(3):755-761.
- 392 Da Silva A.R., Moghaddam M., Liu M., 2014. The future of wireless underground sensing
393 networks considering physical layer aspects. *The Art of Wireless Sensor Networks, Signals and*
394 *Communication Technology*, doi: 10.1007/978-3-642-40066-7-12.
- 395 Di Renzone G., Parrino S., Peruzzi G., Pozzebon A., Bertoni D., 2021. LoRaWAN under-

396 ground to aboveground data transmission performances for different soil compositions. *IEEE*
397 *Transactions on Instrumentation and Measurement*.

398 Ebi C., Schaltegger F., Rust A., Blumensaat F., 2019. Synchronous LoRa mesh network to
399 monitor processes in underground infrastructure. *IEEE Access*.

400 Ferreira C.B.M., Peixoto V. F., de Brito J. A. G., de Monteiro A. F. A., de Assis L. S., Hen-
401 riques F. R., 2019. UnderApp: a system for remote monitoring of landslides based on wireless
402 underground sensor networks. WTIC, Rio de Janeiro, Brasil.

403 Foth H.D., 1990. *Fundamentals of soil science*, 8th edition. Chapter 3, soil physical properties,
404 Wiley, ISBN 0-471-52279-1.

405 Gineprini M., Parrino S., Peruzzi G., Pozzebon A., 2020. *IEEE International Instrumentation*
406 *and Measurement Technology Conference (I2MTC)*, 25-28 May, Dubrovnik, Croatia.

407 Hardie M., Hoyle D., 2019. Underground wireless data transmission using 433MHz LoRa for
408 agriculture. *Sensors*, MDPI, 19, 4232, doi:10.3390/s19194232.

409 Huang H., Shi J., Wang F., Zhang D., 2020. Theoretical and experimental studies on the signal
410 propagation in soil for wireless underground sensor network. *Sensors*, MDPI.

411 Lin K., Hao T., Yu Z., Zheng W., He W., 2019. A preliminary study of UG2AG link quality in
412 LoRa-based wireless underground sensor networks. *IEEE 44th Conference on Local Computer*
413 *Networks (LCN)*, 51-59.

414 Li S., Raza U., Khan A., 2018. How agile is the adaptive data rate mechanism of LoRaWAN?
415 *IEEE Conference and Exhibition on Global Telecommunications*, United Arab Emirates.

416 LoRa Alliance, 2018. *LoRaWAN 1.0.3 Specification*. 1-72.

417 Saeed N., Alouini M.S., Al-Naffouri T., 2019. Towards the Internet of Underground Things: a
418 systematic survey. *IEEE Communications Surveys and Tutorials*, 21(4).

419 Salam A., Raza U., 2020. Current advances in Internet of Underground Things. *Signals in the*
420 *soil*, Springer Nature Switzerland AG, Chapter 10.

421 Salam A., Vuran M.C., Dong X., Argyropoulos C., Irmak S., 2019. A theoretical model of
422 underground dipole antennas for communications in internet of underground things. *IEEE*
423 *Transactions on Antennas and Propagation*, 67(6).

424 Sambo D.W., Forster A., Yenke B. O., Sarr I., Gueye B., Dayang P., 2020. Wireless underground
425 sensor networks path loss model for precision agriculture. *IEEE Sensors Journal*.

426 Staniec K., Kowal M., 2018. LoRa performance under variable interference and heavy multipath
427 conditions. *Wireless Communications and Mobile Computing*, Wiley.

428 Sardar M.S., Xuefen W., Yi Y., Kausar F., Akbar M.W., 2019. Wireless underground sensor
429 networks. *International Journal of Performability Engineering*, 15(11):3042-3051.

- 430 Silva A. R., Vuran M. C., 2009. Empirical evaluation of wireless underground to underground
431 communication in wireless underground sensor networks. IEEE International Conference on
432 Distributed Computing in Sensor Systems, USA.
- 433 Silva A. R., Vuran M. C., 2010. (CPS)2: integration of center pivot systems with wireless
434 underground sensor networks for autonomous precision agriculture. ICCPS, Stockholm, Sweden,
435 10-13.
- 436 Silva A. R., Moghaddam M., Liu M., 2014. The future of wireless underground sensing net-
437 works considering physical layer aspects. The Art of Wireless Sensor Networks, Signals and
438 Communication Technology, DOI: 10.1007/978-3-642-40066-7-12.
- 439 Silva B., Fisher R.M., Kumar A., Hancke G., 2015. Experimental link quality characteriza-
440 tion of wireless sensor networks for underground monitoring. IEEE Transactions on Industrial
441 informatics, 11(5).
- 442 Tiusanen, J., 2009. Wireless soil scout prototype radio signal reception compared to the atten-
443 uation model. Precision Agriculture (10):372-381.
- 444 Trang T. H., Dung L. T., Hwang S. O., 2018. Connectivity analysis of underground sensors in
445 wireless underground sensor networks. Ad Hoc Networks, 71:104-116, 2018.
- 446 Vuran M.C., Akyildiz I.F., 2010. Channel model and analysis for wireless underground sensor
447 networks in soil medium. Physical Communication, 3:245-254.
- 448 Vuran M.C., Silva A.R., 2009. Communication through soil in wireless underground sensor
449 networks, theory and practice. Sensor Networks, Signals and Communication Technology, DOI
450 10.1007/978-3-642-01341-6-12.
- 451 Wu S., Wang K., Ivoghlian A., Austin A., Salcic Z., Zhou X., 2019. LWS: a LoRaWAN wireless
452 underground sensor network simulator for agriculture. IEEE SmartWorld, Leicester, UK.
- 453 Zaman I., Forster A., 2018. Challenges and opportunities of wireless underground sensor net-
454 works. 10.13140/RG.2.2.20241.68968.
- 455 Zorbas D., Papadopoulos G. Z., Maillet P., Montavont N., Douligieris C., 2018. Improving LoRa
456 network capacity using multiple spreading factor configurations. 25th International Conference
457 on Telecommunication, Saint-Malo, France.